Computers and Electronics in Agriculture 224 (2024) 109141

Contents lists available at ScienceDirect

Computers and Electronics in Agriculture

journal homepage: www.elsevier.com/locate/compag

Original papers

Improving 3D reconstruction for accurate measurement of appearance characteristics in shiny fruits using post-harvest particle film: A case study on tomatoes

Mohammad Masoudi [a], Mahmood Reza Golzarian [b,c,*], Shaneka S Lawson [d], Mohammad Rahimi [e], Syed Mohammed Shamsul Islam [c], Rasool Khodabakhshian [a]

[a] Department of Biosystems Engineering, Ferdowsi University of Mashhad, Mashhad, Iran
[b] Harry Butler Institute, Murdoch University, Australia
[c] School of Science, Edith Cowan University, Australia
[d] US Forest Service, Department of Forestry & Natural Resources, Purdue University, West Lafayette, Indiana, USA
[e] Department of Mechanical Engineering, McMaster University, Hamilton, Canada

ARTICLE INFO

Keywords:
Particle film
Photogrammetry
Post-harvest
3D modeling
SFM
Texture

ABSTRACT

Besides the importance of internal quality, the textural quality properties of the product have a remarkable effect on consumer satisfaction and market price. Mainly, the three-dimensional (3D) modeling technique is applied to evaluate the quality of agricultural products. This study aimed to employ the structure from motion (SFM) method along with the particle film technique to predict the physical features of tomatoes. Reconstructing 3D models of tomatoes is challenging due to their shiny skin. In this study, a new method based on particle films was developed to address this issue. Fifty samples of tomatoes were randomly selected with various sizes and four ripeness levels with no-external damage. The SFM technique applied with kaolin particle film was a suitable approach for assessing the surface area, volume, and color index, with a correlation coefficient of 0.76, 0.88, and 0.67, respectively. Also, 3D model predictions achieved these textural properties by obtaining RMSEs of 2.44, 2.30, and 0.35, respectively. Finally, the proposed SFM method's results showed an error of less than 5%. This technique has proven to be a cable technique for the 3D reconstruction of products with a glossy surface.

1. Introduction

Fruit grading is a vital post-harvest operation in fruit processing industries. Accurate product grading is a key factor required to ensure proper marketing of products, especially foodstuffs such as fruit Parameters such as ripeness, shape, texture, size, color, surface de-fects, etc., are scored during fruit grading (Liu et al., 2021; Mon and Zar-Aung, 2020). The first grading step is visual inspection aided by considerable human resources. Moreover, from the viewpoint of cost and time, this step is both time-consuming and costly. Inaccuracy and lacking human resources during meteorological seasons are significant hindrances (Benos et al., 2020; Marinoudi et al., 2019). These issues have compelled the industry to investigate new grading tools. Paramount considerations should be high precision, non-destructive, fast, and cost-effective technologies for detecting and monitoring the quality of fruits and vegetables (Srivastava et al., 2020). Generally, fruit appearance is a prominent feature in quality descriptions (Liu et al., 2021; Naik and Patel, 2017).

Additionally, it is crucial to safeguard the product from detrimental environmental factors. Temperature, among other environmental factors, significantly influences both the quantity and quality of fruit throughout its growth process. For example, tomatoes are sensitive to solar radiation and high-temperature damage (Domis et al., 2002; Dumas et al., 2003). Furthermore, crucial operations include pest control, stress and drought mitigation, as well as safeguarding the product from sunburn. This is during both cultivation and post-harvest storage.

Recently, research has been conducted that measures fruits' geometric characteristics and external quality primarily based on two-dimensional (2D) image processing. Most experimental studies investigated factors such as color, volume, surface area, and dimen-sions of fruits such as apples (Sofu et al., 2016), mango (Thong et al., 2019), bananas (Kipli et al., 2018), citrus (Vivek Venkatesh et al., 2015), apricot (Khojastehnazhand et al., 2019), and tomato (Nyalala et al.,

* Corresponding author.
E-mail addresses: mahmood.golzarian@murdoch.edu.au, mahmood.golzarian@ecu.edu.au (M.R. Golzarian).

https://doi.org/10.1016/j.compag.2024.109141
Received 26 November 2023; Received in revised form 3 May 2024; Accepted 4 June 2024
Available online 24 June 2024
0168-1699/

Nomenclature

SFM	structure from motion
2D	Two dimensional
ΔV	$V_M - V_{3D}$
V_{3D}	Volume assessed by 3D model
ΔA	$A_M - A_{3D}$
A_{3D}	Surface area assessed by 3D model
a^*_{3D}	Red index assessed by 3D model
V_{CMX}	Value of standard cube valume in meshmixer co-ordinate system
A_{CMX}	Value of standard cube surface area in meshmixer co-ordinate system
3D	Three dimensional
V	Volume
V_M	Manual assessed volume
A	Surface area
A_M	Manual assessed surface area
a*	Red/Green value
PLY	Polygon file format
V_{MX}	Value of tomato model valume in meshmixer co-ordinate system
A_{MX}	Value of tomato surface area in meshmixer co-ordinate system

2021) obtained good results.

Advancements in image processing and computer vision methods have eliminated many of the weaknesses of past methods, but limitations still exist (He et al., 2017; Zine-El-Abidine et al., 2021). These conventional techniques are time-consuming, expensive, inaccurate, and may be destructive or semi-destructive for some products. In addition, some of the abovementioned research indicated that geometric shape complexity might decrease the accuracy of 2D image processing. In other words, 2D images are inappropriate predictors of complex three-dimensional (3D) geometric structures (Wang and Chen, 2020). Parameters such as volume, surface area, and color distribution are correctly obtained from 3D geometry of products. Thus, the use of 3D modeling techniques should be considered. Processing of images captured in 2D largely assesses a single view of the product. This leads to a steep decline in measurement accuracy for several parameters (surface area, volume, and color) due to a lack of in-depth information (Jadhav et al., 2019; Paulus et al., 2014). Hence, the development and implementation of 3D reconstruction methods is desperately needed to overcome widespread issues in post-harvest quality assessments. Also, in fields like 3D global mapping, damage recognition, and path planning, 3D reconstruction has numerous applications. One of its applications is helping mobile robots navigate orchards by planning navigation paths and constructing stable fruit-picking robots (Chen et al., 2021; Hu et al., 2024; Ye et al., 2023). The 3D reconstruction methods can be applied using depth sensors such as Microsoft Kinect (Hu et al., 2018; Lin et al., 2021; Yamamoto et al., 2018), Lidar (Hu et al., 2024), and Intel Realsense (Chiang and Fan, 2018; Herak et al., 2018). Depth sensor usage is often time-consuming, expensive, and has a limited working range. Techniques such as stereo vision (Abd Rashid et al., 2020; Malekabadi et al., 2019) and structured light (Sarafraz and Haus, 2016) have been also employed for 3D reconstruction. The primary limitation for bother stereo vision and structured light is the inability to generate 360° object views, thus, reducing the accuracy of some parameter estimates. In recent years, neural network-based and deep learning methods have emerged as powerful tools for acquiring 3D data from 2D images. These advanced techniques have demonstrated significant potential in various applications and continue to drive innovation in the field (Feng et al., 2020; Kench and Cooper, 2021; Li et al., 2023).

Furthermore, in recent years, the use of particle films has emerged as a novel approach, which has demonstrated highly promising results. It has long been known that particle films are capable of mitigating the effects of water and heat stress on agricultural products. This technology was originally developed for pest control purposes (Saavedra Del R et al., 2004).

The use of a kaolin-based particle film improves fruit quality, controls certain pests, and reduces heat stress (Glenn and Puterka, 2010). Kaolin forms a protective layer on the fruit, which reduces water consumption. Many research reports emphasize the beneficial effects of kaolin on sunburn damage in fruits such as pomegranates, apples, walnuts, citrus fruits, and tomatoes (Boari et al., 2015; Cantore et al., 2009; Glenn, 2012; Pace et al., 2006; Saavedra Del R et al., 2004; Weerakkody et al., 2010).

Gharaghani et al. (2018) conducted research that revealed the use of kaolin particle film reduces the adverse effects of light and heat stress, while improving the quality of walnut kernels. Additionally, Sharma et al. (2020) stated that kaolin-based particle sprays reduce pests, diseases, and storage disorders, enhancing the post-harvest quality of apples.

Furthermore, Palma et al. (2020) examined the effects of kaolin particle film on physiological parameters, nutritional composition, nutrients, and Ceratitis capitata infestation in peach fruits during harvest and storage. The results indicated a significant reduction in medfly attacks on kaolin-treated fruits (0.5 % damaged fruits) compared to untreated samples (10 % damaged fruits).

The structure from motion (SFM) technique is one of the most popular 3D reconstruction processes developed in recent years. This process initially utilizes computer vision techniques to isolate key features before estimating 3D structure of the object, camera position, and location from multiple collected images. These functions lead to the creation of a fully reconstructed 3D model. In addition, SFM is accurate, cost-effective, and easily accessible (Edelman and Aalders, 2018). The advantages and abilities of SFM make it a superior technique compared with other image processing methods. SFM has successfully estimated the physical characteristics of agricultural products such as bell pepper plants (Ayob et al., 2015), strawberries (He et al., 2017), apples, mangoes, oranges, pomegranates (Jadhav et al., 2019), and trees (Miller et al., 2015). Mainly, SFM technique has been widely adopted in practical, real-world engineering applications, including agriculture (Meinen and Robinson, 2020) and forestry (Iglhaut et al., 2019). These studies have showcased promising results, highlighting the efficacy and versatility of SFM in various domains.

A challenge with this method is the accurate representation of monochromatic objects and those with polished, reflective, semi-glossy, or shiny surfaces (Aldeeb and Hellwich, 2018; Hosseininaveh Ahmadabadian et al., 2019). Researchers have tried several approaches to overcome this hindrance from the projection of random patterns on the object (Ahmadabadian et al., 2013), image enhancement (Aldeeb and Hellwich, 2018), and using a marker to outline specific areas (Aguilar et al., 2007). Unfortunately, these potential solutions require costly equipment and complex calibrations by an expert in photogrammetry and computer vision. While methods like structured light excel in reconstructing objects with insufficient surface texture and smooth surfaces, they are not without limitations. This approach necessitates sophisticated and costly equipment, entails computationally intensive operations, demands precise calibration of both the camera and projector, and falls short in generating a comprehensive 360-degree global model of the object. When compared to other 3D reconstruction techniques like laser scanners, depth sensors, and structured light, SFM offers advantages such as simplicity, lower computational cost, and more accessible equipment. Given these benefits and the constraints of our study, the SFM method was deemed the most suitable approach for our research. One fruit challenging to image with SFM, and the subject of this manuscript, is tomatoes. This work presents a non-destructive solution using SFM for the 3D reconstruction of tomatoes with polished, reflective, and shiny surfaces. Fig. 1 illustrates an example of particle film technology applied to tomato fruit.

The method proposed in this study addresses the limitations of the Structure from Motion (SFM) technique in reconstructing samples with the mentioned characteristics. In addition to overcoming the constraints of this technique, it yields positive effects on post-harvest processes and product preservation during growth and storage periods. In the presented method, a particle film is created on the surface of the fruit, which not only adds key properties to the product's surface but also forms a protective layer on the fruit. The particle film is typically sprayed onto the fruit while it is still on the tree or bush. Here, we will perform this procedure under controlled conditions on a single fruit in the laboratory. Our literature review revealed that the application of the SFM technique in agriculture and horticulture has been restricted due to certain limitations. In this study, we aimed to address some of these limitations and expand the technique's utility in these sectors. The innovative aspect of our research lies in the use of the particle film technique to enhance the 3D reconstruction of products with shiny and polished skin using SFM. This novel approach not only improves the accuracy of 3D reconstruction and estimation of physical parameters but also leverages the properties of the kaolin film, which have been demonstrated in previous studies to extend the shelf life of products during post-harvest and storage periods. It is important to note that the scope of our research was conducted in a laboratory setting and offline.

Here, the measurement of appearance characteristics with sensitive surface texture characteristics such as color index, surface area, and volume was facilitated by dusting the product surface with kaolin particle film before imaging. The particle film method was compared with other preparation techniques: marking and labeling. Tomato samples were collected at four different ripeness levels, and their stem and calyx parts were removed. Subsequently, a kaolin particle film was applied to the samples for the particle film method, while markings and labels were used for the other two preparation methods. The necessary images were then acquired, and the 3D models of the samples were reconstructed using the SFM method. Finally, physical parameters were estimated, and the accuracy of the proposed particle film method was evaluated in comparison to the marking and labeling techniques.

2. Material and method

2.1. Samples

Red tomatoes were collected from a produce farm located on the campus of Ferdowsi University in Mashhad, Iran. The evaluation process

Fig. 1. Showcases tomatoes treated with kaolin clay to mitigate stink bug damage. (Source: University of Maryland Extension, "Stink Bugs in Vegetables").

was comprehensively illustrated in Fig. 2. Depicts the flowchart illustrating the sequence of processes applied to the images leading to the construction of a 3D model fifty tomato samples were tested using the SFM method to gauge the accuracy of the 3D modeling method. Undamaged tomatoes at four levels of ripeness: unripe (green), turning (green-yellow), semi-ripe (yellow-orange), and fully ripe (red) with 14, 15, 17, and 19 weeks from planting, respectively, were selected for further study. Each sample was preparated with kaolin particle film after the removal of the calyx. The calyx part was meticulously removed using tweezers to ensure minimal disruption to the sample (Fig. 2g).

2.2. Assessment of sample volume, surface area, and color index

The water displacement method is a typical and straightforward method to assess volume in fruits and vegetables. This technique was used here following the protocols of a surface area determined by the peeling method (Omid et al., 2010) and the photoshop (Adobe, Inc) software suite. The color index was also ascertained using Photoshop combined with MATLAB® software and standard image processing. A color calibration tool for cameras called ColorChecker® X-Rite ColorChecker Passport (Calibrite®, Wilmington, DE) was used to boost accuracy (Steeper, 2012). This index was derived exclusively for tomatoes as the L*a*b* color space definition of tomato ripeness is the a* index. In the RGB color space, it is not possible to detect color accurately. To overcome this limitation, each RGB image is converted to a Lab image. Among the components of the Lab color space, the a* component has been found to be the most reliable for estimating tomato maturity. Therefore, the authors extract features using the a* component. The tomato maturity is determined by calculating the mean values of the a* components within the tomato region. As the a* value increases, the tomatoes exhibit more redness and ripeness (Rupanagudi et al., 2014). The a* index ranges from −128 to +128, with higher values indicating a redder and riper tomato as it matures. Table 1 provides a summary of key parameters and their corresponding descriptions relevant to the study.

2.3. Sample preparation

A roller carrier and a 200 mesh pulse sieve were used in sample preparation and particle film generation. For sample preparation, fine mesh kaolin powder was used. The size of kaolin particles is mainly in the range of 25–35 μm (Yahaya et al., 2017). Each tomato was gently rinsed with water and thoroughly dried with a soft cloth towel. After reaching the end of the vibrating movable component, the tomato sample was securely but gently held for image processing in an imaging frame (Fig. 2). The methodologies for marking and labeling follow a similar workflow to the kaolin particle film technique, as illustrated in Fig. 2. The only difference among these methods lies in the preparation stage (Fig. 2b), where marking with a marker and affixing labels replace the particle film application. For this purpose, a whiteboard marker and colored labels were employed. It is noteworthy that marking and labeling techniques generally do not follow a specific pattern or approach, as no particular method was identified in the reviewed literature. In summary, the marking method involves creating unique patterns on the object's surface using a whiteboard marker, while the labeling method utilizes colored labels to create similar patterns. Despite the differences in implementation, both techniques serve to enhance surface features for improved 3D reconstruction using SFM.

2.4. Image capture

Photographs were obtained using a digital camera, a graduated manual turntable, a sample stabilizer, an imaging chamber, and LED USB lamps (USB LED28). The 3D sample reconstruction was performed with SFM. To ensure adequate data was provided, images from different sample angles were collected. The SFM algorithm, based on recognizing,

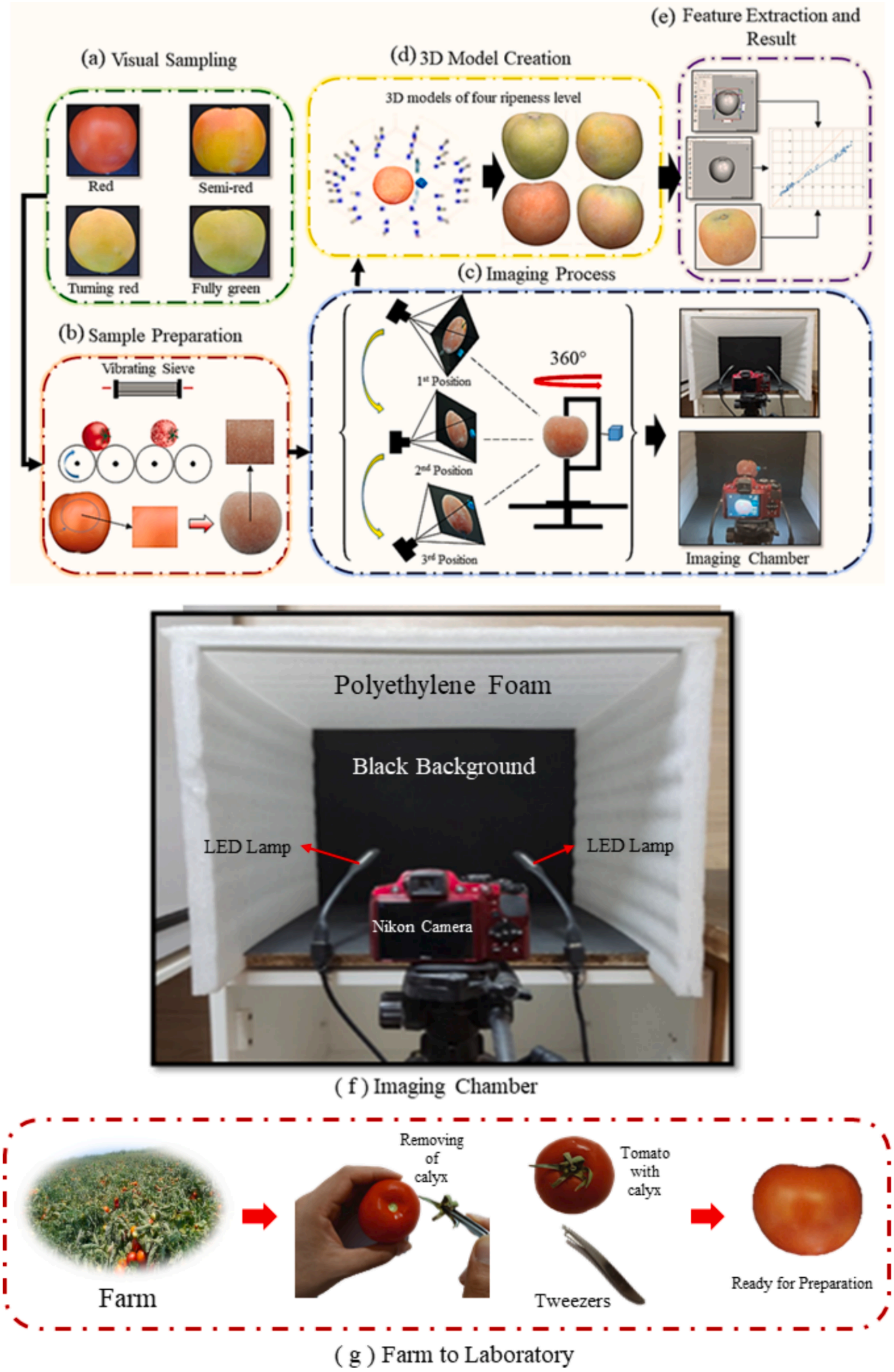

Fig. 2. A schematic representation illustrating the key processes involved in the current study, including sampling, setup preparation, data acquisition, and 3D reconstruction processes.

extracting, and matching key image features between photo was applied. To ensure the most exacting photos were collected, an imaging chamber, a turntable, and a stabilizer were engineered. The turntable had a 75 mm radius, a 50 mm height, and was spray-painted matte black in color (Fig. 2c). A sample holder was engineered to minimize contact surface and maximize the visibility of the surface area available for photographing. Fewer obstructions improve 3D reconstruction accuracy. The imaging chamber (Fig. 2f) size was 350 x 350 x 350 mm^3. A black background was used to eliminate shadows. The chamber ceiling and walls were covered with polyethylene foam (20 mm thick) to avoid the effect of ambient light while two USB LED lamps (1.2 W) (Fig. 2c) were used to illuminate the lowest portion of the sample. A Nikon Coolpix P510 camera (Nikon Inc, Japan) was used for imaging and a laptop with an Intel Core i5, 4200 M, 2.5 GH processor, and 6 GB

Table 1
Summary of key parameters and their decriptions.

Symbol	Feature
V	Volume (cm^3)
V_M	Manual assessed volume (cm^3)
A	Surface area (cm^2)
A_M	Manual assessed surface area (cm^2)
a*	a* chromatic color component in L*a*b* color space
a^*_{3D}	a* chromatic color component in L*a*b* color space assessed by 3D model

of RAM was used for data processing. The locations of the equipment remained constant throughout the imaging to prevent variation in photo capture distance between images. Once affixed to the stabilizer, each tomato was imaged from three positions (upper, middle, and lower), with an image taken every 30 degree turn of the turntable to ensure full coverage. This resulted in 36 images being obtained for each sample (Fig. 2c) with the sample so that all parts of the sample were covered.

2.4.1. Standard cube

A standard 1 cm^3 cube were placed next to the target tomatoes (Fig. 2c) to provide a size reference during sample reconstruction. Image features were pieces of local information in an image, and they were used to find correspondences in paired images and help in recovering the camera parameters in a 3D scene (Miller et al., 2015). As a result, the parameters of cameras, such as position and orientation, cannot be correctly recovered, which may result in apparent errors in the generated point clouds. On the other hand, due to the regular square shape, the image features (usually located at corners or edges of each square) can be easily detected by feature detection algorithms. These image features provided additional correspondences and led to more accurate and stable point clouds (Fuhrmann et al., 2015).

2.5. Point cloud reconstruction

3D point clouds were receonstructed of the features extracted from the 2D images of tomato samples, acquired by the imaging system described in section 2.4. The reconstruction process employed in this study consists of three main steps (Fig. 3): i) image preprocessing, ii) 3D point cloud reconstruction, and iii) post-processing of the point clouds (Fuhrmann et al., 2015). These steps were executed through codes and alagorithms using Computer Vision toolbox of MATLAB (Ver 2020b, Mathworks inc, US). Each step is explained as follows:

2.5.1. Image processing

The main operation in preprocessing step is background removal. To achive this, the images were filtered using Gaussian filter to eliminate random noise. Susbequently, they were converted from the RGB space to the HSV color space. The HSV color image was then thresholded and converted to a binary image, where pixels corresponding to tomato regions were assigned as 1 (white) and those associated with the background were set to zero (black). In this work, the threshold values of H (hue), S (saturation), and V (value) channels were 0.4, 0.1, and 0.1, respectively. By overlaying this mask onto the original color image, we obtain the image of tomato with the background was effectively removed (Fig. 3a). In this paper conversion (from RGB to HSV) requires the following steps (Chernov et al., 2015):

1. Find maximum (M) and minimum (m) of R; G, and B.
   $M = \max(R,G,B)$
   $m = \min(R,G,B)$
2. Assign V = M.
3. Calculate delta (d) between M and m.
   $d = M - m$
4. If d is equal to 0 then assign S with 0 and return. H is undefined in this case.
5. Calculate S as a ratio of d and M.
6. Calculate H depending on what are M and m.

2.5.2. 3D reconstruction

In this study, the SFM technique extracts homologous points from the collected images, enabling the derivation of three-dimensional information for the samples. The input to the SFM technique is pre-processed images obtained from various angles of the target object, here tomato samples. Initially, the Scale-Invariant Feature Transform (SIFT) algorithm (Lowe, 2004) was applied to extract key features from the images. Camera parameters such as Orientation and Position were recovered by matching corresponding key features of the images. Subsequently, using the recovered parameters, a Sparse point cloud was generated. Then, a depth map for each image was created by calculating the depth information of each pixel. The dense point cloud was then generated by merging all the depth maps. Finally, the Fast Screen and Shape Recognition (FSSR) algorithm (Fuhrmann and Goesele, 2014) was used to denoise the dense point cloud (Fig. 3b). Fig. 4 provides a schematic representation and flowchart detailing the SFM technique employed in this research.

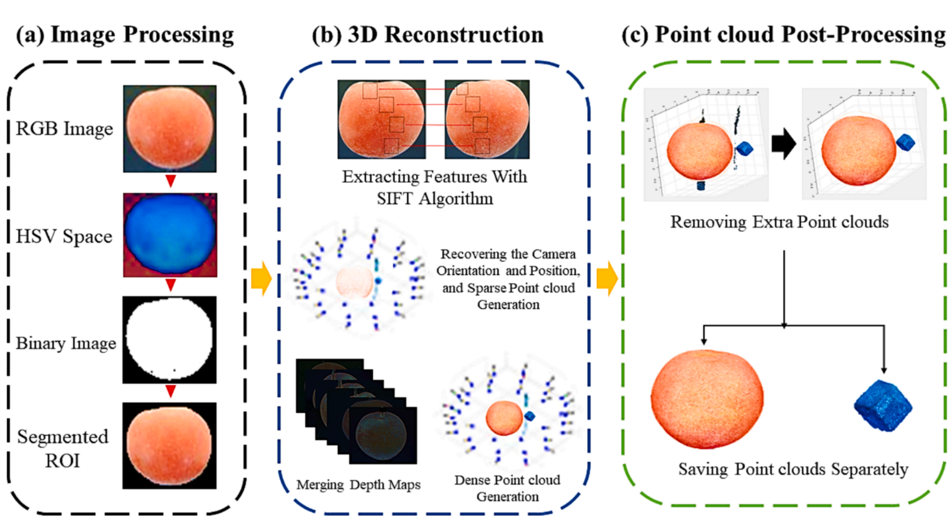

Fig. 3. The reconstruction process: a) image processing, b) 3D reconstruction, and c) Point cloud post-processing.

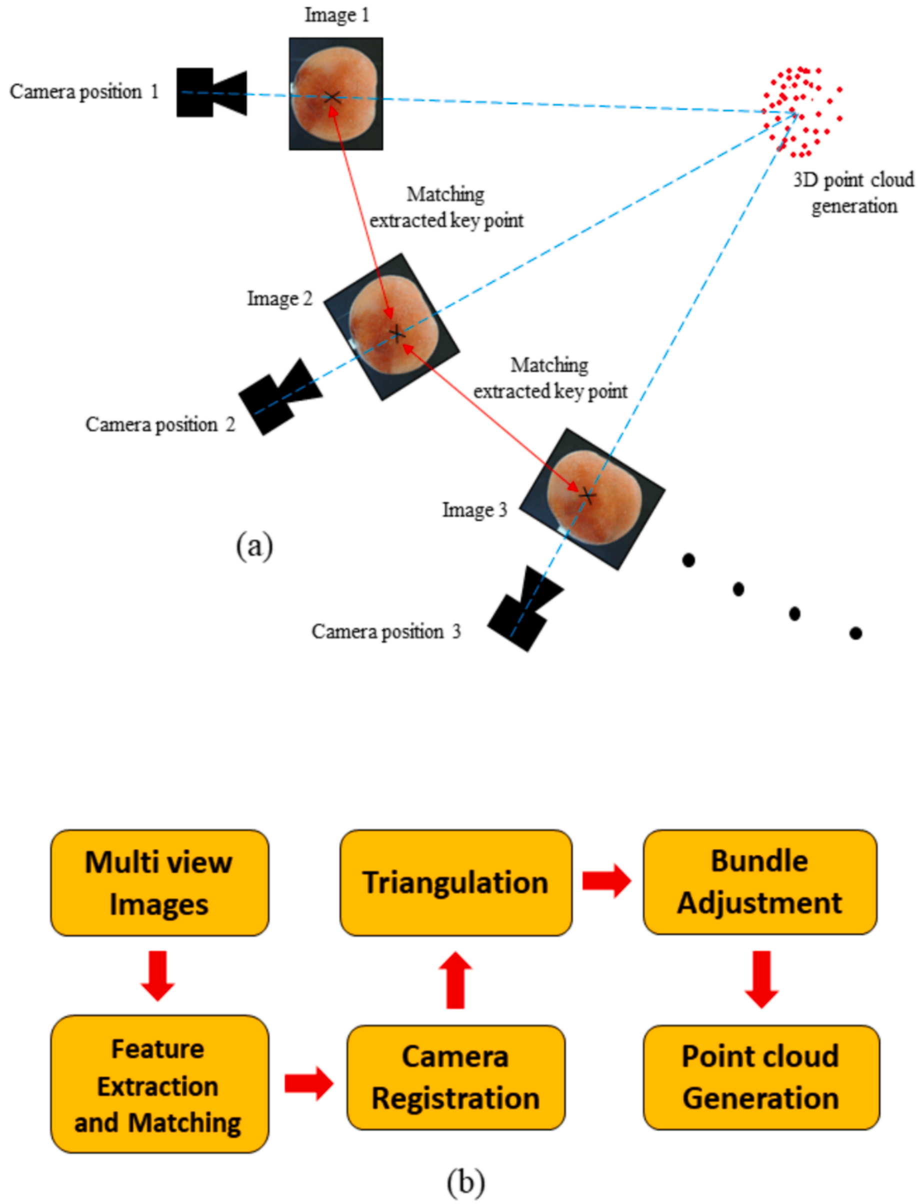

Fig. 4. Schematic representation and flowchart of the Structure from Motion (SFM) technique, illustrating (a) the process of key point extraction and matching, and (b) the algorithm utilized for 3D point cloud generation.

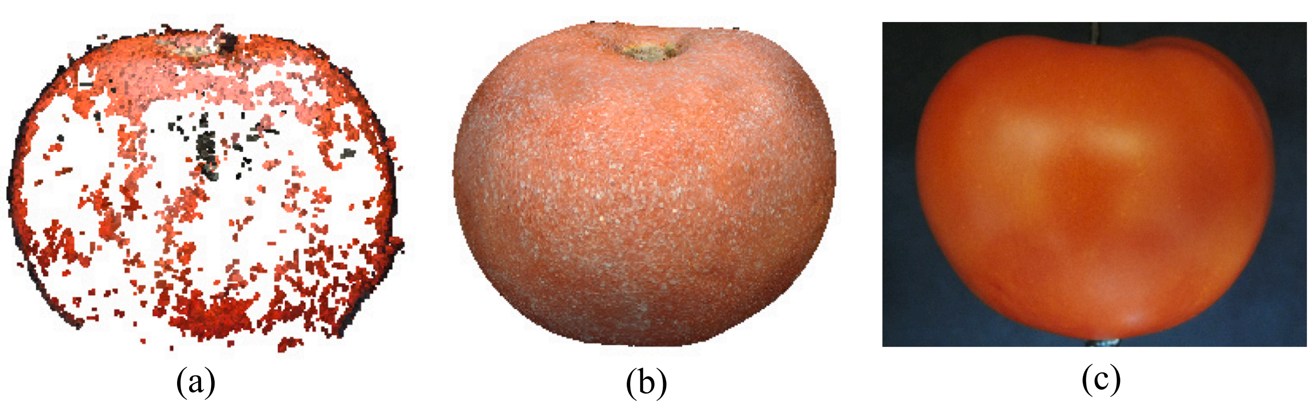

Fig. 5. Comparison of 3D model reconstructions (a) prior to making kaolin particle film (without preparation), (b) after making kaolin particle film (with preparation) and (c) image of the measured tomato.

2.5.3. Point cloud Post-Processing

Since the 3D model of tomatoes and standard cubes are our objects of interest, other reconstructed elements of the scene, such as the holding clamps, were removed. This process consists of two steps: First, the tomato and the reference cube were segmented from the background in each dense point cloud. To achieve this, the G-DBSCAN algorithm (Andrade et al., 2013), which is a 3D clustering algorithm, was applied to the de-noised point cloud obtained after application of SFM technique. This algorithm was adapted from the "pcsegdist" function in MATLAB. This functions utilizes Euclidean distance parameter in clustering. Subsequently, criteria were defined to identify points related to the target, and the target point cloud was segmented from the rest of the scene components. This process was repeated twice for the point cloud set: first, tomato points were considered as the target and second time, the reference standard cube as the target. The output of the point cloud post-processing were two separately saved point cloud of tomato and standard cube. From these point cloudes, physical parameters were extracted (Fig. 3c).

An example of these process results is shown in Fig. 5. The poorly reconstructed point cloud is expected as the precision of SFM decreases when image subjects are polished, shiny, or reflective and lack surface texture characteristics. Thus, the optimal performance of SFM is compromised as the algorithm's ability to extract key points, match them, and estimate depth suffers. Also, bright spots on the surface will alter the algorithm's performance in cases of shiny or polished subjects. Thus, the kaolin particle film effectively donates high ability to the SFM technique.

2.6. 3D model analysis

Meshmixer (Autodesk Meshmixer, Autodesk Inc., San Rafael, USA) software was used to estimate volume and surface area of the 3D models (Herak et al., 2018). To begin, the standard cube model was loaded into the software and values for volume and surface area were calculated with the process repeated for the sample. Because parameter values are given for the standard cube, the volume and surface area of the sample model can be calculated. In **Eqs. (1) and (2)**, the method of estimating the volume and surface area is presented, respectively. Where V_{3D} is the estimated volume of the sample, V_{MX} is the volume of the sample model, V_{CMX} is the volume of the standard cube model. Also, A_{3D} is the estimated surface area of the sample, A_{MX} is the surface area of the sample model, A_{CMX} is the surface area of the standard cube model.

Also, by using MATLAB software, color index can be derived. The RGB data of all points (point clouds) was extracted and converted into L*a*b* color space (also referred to as CIELAB (International Commission on Illumination color space)). L*a*b* is a three-value description of color where L* corresponds to perceived light while a* and b* represent the four distinct colors in the range of human vision: red, green, blue and yellow. In this work, the a* channel is discredited and its average calculated before being given as the color index of the 3D model. With our hardware setup, the time required for acquiring the images, processing and extracting the information was 60 s, 5 s and 10 s, respectively.

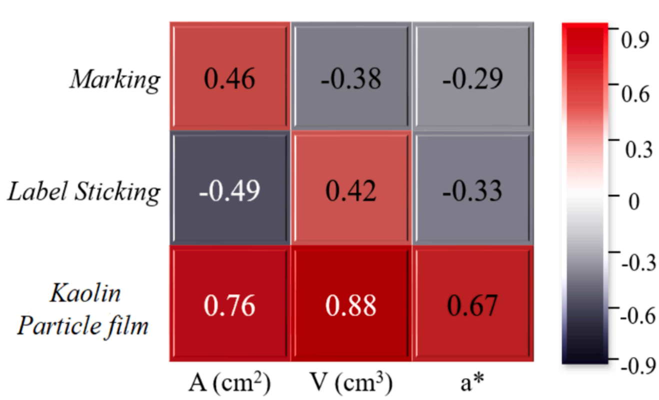

Fig. 6. PCC matrix achieved between the preparation methods and physical features.

$$V_{3D} = \frac{V_{MX}}{V_{CMX}} \quad (1)$$

$$A_{3D} = \frac{6^{*}A_{MX}}{A_{CMX}} \quad (2)$$

2.7. Pearson correlation coefficient (PCC)

For comparison of the 3D model, the Pearson correlation coefficient (PCC) was ac-complished to evaluate the correlation between extracting physical features and preparation methods. The PCC was applied to evaluate the collinearity value between physical var-iables and preparation methods. The existence of linear dependence is determined as **Eq. (3)** (Rahimi et al., 2022):

$$\rho_{xy} = \sum_{i=1}^{n}(x_i - \bar{x})\sum_{i=1}^{n}(y_i - \frac{\bar{y})}{\sqrt{\sum_{i=1}^{n}(x_i - \bar{x})^2}\sqrt{\sum_{i=1}^{n}(y_i - \bar{y})^2}} \quad (3)$$

where x and y represent preparation methods and three detected physical features while $\bar{x}$ and $\bar{y}$ are their mean values. **Eq. (3)** varies between −1 and 1, which is constant to the linear conversion, therefore: $\rho_{xy} = -1$, 0, and 1 represent x and y have completely negative, obscure, and positive correlations, respectively. Moreover, the correlation coefficient discloses the significant levels that are calculated as **Eq. (4)**:

$$t = \frac{\rho_{xy}\sqrt{N-2}}{\sqrt{1-{\rho_{xy}}^2}} \quad (4)$$

P-value is achieved by calculating the "t" distribution by degrees of freedom (equal to N-2). These conceptually exhibit the impact propensity of the input variable on the output variable as a primary test. Here PCC is used as primary statistical analysis to disclose the 3D reconstruction technique.

2.8. The performance criteria

Two performance functions utilized to analyze the accuracy of the SFM technique such as R^2 and Root MSE (RMSE) are defined as **Eqs. (5) and (6)**:

$$R^2 = 1 - \left(\sum_{1}^{N}(X_a - X_p)^2 \Big/ \sum_{1}^{N}(X_a - \widehat{X}_r)^2\right) \quad (5)$$

$$RMSE = \sqrt{\left(\sum_{a=1}^{N}|X_a - \widehat{X}_p|^2\right) \Big/ (N-1)} \quad (6)$$

where X_a and X_p are the actual and the predicted values, respectively. $\widehat{X}_r$ and $\widehat{X}_p$ are displayed the average of the actual values.

To evaluate the repeatability of the preparation method, the coefficient of variation (CV) was employed, defined as the ratio of the standard deviation (σ) to the mean (μ), as shown in **Eq. (7)**:

$$CV = \frac{\sigma}{\mu} \quad (7)$$

Table 2
Results of compare means test for four different levels ofripeness (ANOVA table).

			Sum of Squares	df	Mean Square	F	Sig.
Color Index * Ripeness	Between Groups	(Combined)	45280.702	3	15093.567	920.156	0.000
	Within Groups		1115.422	68	16.403		
	Total		46396.124	71			

3. Results and discussions

3.1. Primary statistical analysis

Samples ranged in volume from 31.80 cm^3 to 160.70 cm^3, surface area from 49.65 cm^2 to 169.40 cm^2, and color index (a*) values from −12 to 58.32. The large spread in recorded data seen for these parameters is expected and is indicative of an even distribution of tomatoes chosen for analysis and a wide variation in tomato size and shape. The accurate analysis of tomatoes of assorted sizes demonstrates the many possible objects that can be imaged effectively.

Three preparation methods for 3d reconstruction technique are evaluated based on the correlation criteria in comparison with extracted physical features of tomatoes. As shown in Fig. 6, the particles film method displayed a significant correlation with the surface area, volume, and color index extracting with significant levels (p-value) of <0.01. Particles film technique was positively correlated with the correlation coefficient of 0.76, 0.88, and 0.67, respectively. Marking and labeling preparation methods exhibit a non-significant level and weak correlation for physical feature extraction. These results show that the particle film technique has a much smaller effect on the estimated volume and surface area of the sample than the other two techniques (marking and labeling). This is due to the significant improvement in the quality of the 3D reconstruction of the sample by combining the SFM method and the particle film technique compared to the other approaches. Also, according to the results, the volume has the least effect from the particle film technique and the greatest effect was on the estimation of the color index, which could be due to the white color of the kaolin powder, which affected the extracted color index.

The runs test was applied to validate the randomness of sampling and the K-S (Kolmogorov–Smirnov) test was used to assess the normality of the data. Also, the compare means test was conducted to examine the significance of the difference in the color index for four different levels of ripeness. According to the results, since sig >0.05 for both the runs test (sig $=$ 0.059) and the K-S test (sig $=$ 0.115), the null hypothesis cannot be rejected at the 95 % confidence level. This indicates that the sampling was random and the sample distribution was normal. Also, according to Table 2, since the sig <0.05 (sig $=$ 0.000), the null hypothesis is rejected at the 95 % confidence level, implying that the average color indices of the different ripeness levels exhibited significant differences, highlighting the substantial variation in ripeness and color among the samples.

3.2. Statistical comparison of sample preparation methods

Three various preparation techniques were applied to the tomato sample. Although SFM is a powerful method, its performance can be compromised by an object's surface characteristics. Surface characteristics refer to the presence of distinct features on the product's surface, such as spots, roughness, or color variations across different sample surface regions. These characteristics play a crucial role in the performance of the SFM method since the technique relies on extracting key surface features. Consequently, lacking such characteristics may hinder the SFM method's effectiveness, making it more challenging to achieve accurate 3D reconstructions. Thus, in cases where an object lacks suitable features, these traits must be artificially generated. Various approaches and preparations were tested on a tomato sample with illustrations of the 3D reconstruction efforts shown in Fig. 7. This figure serves as a visual depiction showcasing the impact of various preparation methods on the performance of the Structure from Motion (SFM) technique. It outwardly illustrates the influence of three distinct preparation strategies on the SFM technique's effectiveness. Specifically, this graphical representation clearly demonstrates the significantly superior performance achieved through the implementation of the particle film method compared to alternative preparation methods.

These methods prominently display their performances to estimate the three textural features, including surface area, volume, and color index. For evaluationg the performance of the preparation methods, a tomato sample with a volume of 104.86 cm^3 and a surface area of 113.58 cm^2 was tested using the preparation techniques and the results of physical features are presented in Table 3. The number of images obtained for all methods was uniform. For the method involving random hand-drawn markings on the tomato, the volume estimation error was 9.37 %, the surface area estimation error was 9.97 %, and the color index error reached 37 %. When colored labels were affixed to the surface, the volume estimation error was 9.14 %, the surface area estimation error was 11.09 %, and the color index error decreased to 25.55 %. In contrast, the proposed particle film method achieved significantly lower errors, with a 1.54 % error for volume estimation, 2.16 % for surface area estimation, and 4.7 % for color index estimation. Moreover, the particle film method demonstrated strong performance with R-squared (R^2) values of 0.98, 0.97, and 0.90 for volume, surface area, and color index, respectively.

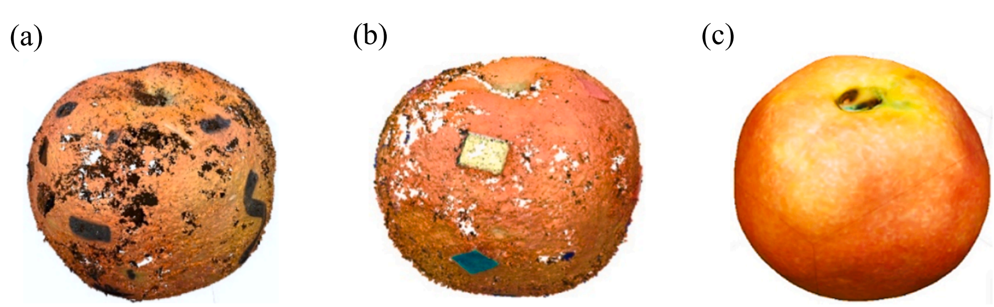

Fig. 7. The results of 3D modeling with different preparation methods,)a) Marking, (b) Labeling, (c) Kaolin Particle film.

Table 3
Comparison of extracted physical features for sample preparation methods.

Preparation method	V(cm^3)			A(cm^2)			a*		
	ΔV (cm^3)	Error %	R^2	ΔA (cm^2)	Error %	R^2	Δa*	Error %	R^2
Marking	9.83	9.37	0.80	11.33	9.97	0.81	4.49	37	0.40
Labeling	11.05	9.14	0.76	12.60	11.09	0.79	3.1	25.55	0.56
Kaolin Particle film	1.62	1.54	0.98	2.46	2.16	0.97	0.57	4.7	0.90

Table 4
Evaluation of the proposed preparation method (Kaolin Particle Film).

Sample	Repeat	V_M	V_{3D}	ΔV	A_M	A_{3D}	ΔA	a^*_{3D}
Red	1	88.32	90.11	1.79	104.18	107.37	3.19	11.71
	2		90.24	1.92		107.91	3.73	12.88
	3		89.58	1.26		107.43	3.25	12.28
Semi-red	1	78.14	79.22	2.21	78.23	81.12	2.12	10.51
	2		80.35	1.92		80.78	3.03	9.68
	3		80.17	1.26		80.21	2.65	10.13
Turning red	1	65.31	67.54	2.23	86.45	88.36	1.91	8.51
	2		67.9	2.59		88.19	1.74	7.93
	3		67.14	1.83		88.72	2.27	7.35
Fully green	1	85.4	88.12	2.72	98.36	102.15	3.79	2.16
	2		86.9	1.5		102.43	4.07	2.42
	3		87.45	2.05		101.94	3.58	2.3

3.3. Evaluation of preparation method

The primary obstacle to overcome has been reduction of sample surface reflection with artificial enhancement of surface texture. This newly described protocol reduces operator impact and has the added benefit of being repeatable. The novel addition of a kaolin particle film to the entire sample surface dramatically improved accuracy. To verify repeatability, four tomatoes were randomly selected and analyzed three times each. Also, the results of this proof of concept step are shown in Table 4. The results of our analysis showed that the average coefficient of variation (CV) was 0.54 % for volume estimation and 0.26 % for surface area estimation, indicating a low degree of variability in these measurements. However, the CV for color index estimation was found to be 5.87 %, suggesting a higher degree of variability in color index estimation compared to the other parameters.

3.4 Volume. , surface area, and color index estimation

The SFM technique was used to create 3D surface reconstruction models of 50 tomatoes, and the parameters (volume, surface area, and color index) were measured. The results of the linear regression analysis performed on the estimated and measured tomato values are observed. The root means square error (RMSE) criteria were used to estimate the result of the linear regression analysis. Fig. 8 represents the manually measured values in the x-axis, and the y-axis exhibits the estimated values computed using the SFM technique. The best-fit line of this distribution is named the "45-degree line", which indicates a satisfactory prediction and 3D model performance of the SFM technique. The tomato size distribution range is vast and homogeneous (as can be seen in Fig. 8). There is a high correlation between the estimated values and the actual measured values of tomato parameters. The slope of the regression line for volume and surface area is also near 1, and both are approximately on the ideal regression line (Y = X), as shown in Fig. 8a and b. The RMSE for estimating volume was 2.30, and for the prediction of surface area was 2.44. The acquired data showed that the suggested approach accurately assessed the volume and surface area of tomato samples with 98.02 % and 98.28 % accuracy, respectively. This error might be attributed to the non-uniform thickness of the particle film on certain parts of the sample surface. To investigate the influence of the kaolin particle film on sample color, the samples were divided into training and testing groups, comprising 70 % and 30 % of the samples, respectively. Training data were used to generate Fig. 8c. the color index

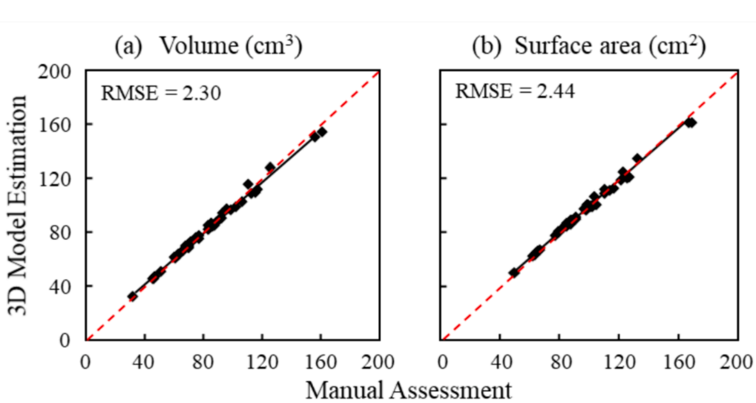

Fig. 8. Regression study of (a) volume, (b) surface area, and (c) color index as determined by manual and 3D model evaluation. Red lines represent ideal regression curves (y = x), and black lines are least squares linear regression curves.

Table 5
The results of evaluating the effect of adding kaolin powder on the color index of the samples.

Sample	a* (3D model)	a* (diagram equation)	a* (manual assessing)	RMSE
1	−6.40	−6.15	−7.09	**0.59**
2	−7.51	−7.64	−7.67	
3	−4.22	−3.23	−3.21	
4	−7.71	−7.91	−5.96	
5	−4.98	−4.25	−2.18	
6	−0.41	1.87	1.98	**0.30**
7	0.26	2.77	3.86	
8	−1.97	−0.21	0.80	
9	−0.49	1.76	2.07	
10	9.35	14.95	15.00	
11	20.87	30.40	27.97	**0.82**
12	18.54	27.28	27.72	
13	28.74	40.95	39.07	
14	25.15	36.14	37.93	
15	21.17	30.80	32.88	
Total	–	–	–	**0.35**

by SFM technique achieved 0.35 of RMSE.

This would clearly illustrate how the ‘dusting’ procedure (making particle film on sample) impacted sample color. Graphing the training data, Fig. 8c, revealed a distortion in the 3D renderings of tomatoes where a* increased (greater intensity of redness) resulted from dusting the samples. The rendered colors for test samples chosen at random were estimated and compared with their manual values (Table 5). Additionally, the RMSE error value for color estimation was determined to be 0.59 for green, 0.30 for yellow-orange, and 0.82 for red samples while the combined RMSE value for all test samples was 0.35. Table 6 presents the results of comparable studies and practical applications in real engineering scenarios, demonstrating that our findings align well with those of previous research, further highlighting the potential of our method for a range of engineering applications.

4. Conclusion

In this survey, the performance of the SFM technique as an efficient method for the 3D reconstruction of tomatoes with reflecting and glossy surfaces were examined. In this study, an innovative approach based on particles film was used to overcome the limiations of the Structure from Motion (SFM) technique for reconstrcting a 3D models of shiny agricultural products. This approach not only improves the reconstruction of the three-dimensional tomato model, but it also serves as a shield, guaranteeing the maintenance of product quality both during and after harvest. Three physical features such as the surface area, volume, and color index of tomatoes were extracted and 3D modeled by the SFM method with particle film technique. It exhibits higher efficient performance compared with marking and labeling methods. These two preparation methods failed by PCC (low correlation coefficient), statistical analysis (p-value > 0.1), and output media. SFM with kaolin particle film positively exhibited a higher correlation in the range of 0.67 to ∼0.9 with a p-value < 0.01. SFM achieved a 3D model based on the surface, volume, and color by obtaining the RMSEs of 2.44, 2.30, and 0.35, respectively. SFM method usefully conducted a 3D model for tomatoes as a glossy product. In general, the SFM method, as a cheap 3D imaging technique, can be used to evaluate the geometrical characteristics, texture, and color of products with different surface characteristics and obtain favorable results. In future studies, to transition this technique from laboratory conditions to real-world engineering applications, the impact of environmental factors, such as shadows and lighting, as well as advanced 360-degree imaging technologies, could be examined. By addressing these factors, the limitations of the method can be reduced, and its scope of application expanded within various agricultural sectors, including product monitoring, harvesting robots, and surveying drones. A key limitation of this research lies in the time-consuming imaging process and its laboratory setup. Note that the present study was conducted in a controlled laboratory environment to primarily investigate the effects of particle film coating on the quality of 3D reconstruction for products with shiny surfaces. In subsequent research phases, external factors could also be incorporated. Future studies may focus on the application of this method as an accurate, affordable, and accessible means to evaluate various products with diverse geometrical textures, colors, and reflective surface properties. Also, using microscopic coatings to improve three-dimensional reconstruction, even the effect of starch on tomato physical properties and storage time can be investigated.

CRediT authorship contribution statement

Mohammad Masoudi: Writing – original draft, Software, Methodology, Formal analysis, Data curation. **Mahmood Reza Golzarian:** Writing – review & editing, Writing – original draft, Visualization, Supervision, Project administration, Methodology, Investigation, Formal analysis, Conceptualization. **Shaneka S. Lawson:** Writing – review & editing, Validation, Supervision, Methodology. **Mohammad Rahimi:** Writing – original draft, Software, Methodology, Formal analysis, Data curation. **Syed Mohammed Shamsul Islam:** Writing – review &

Table 6
Review of 3D Reconstruction Methods in Agriculture and Animal Husbandry Industry.

Product	Application	Model	Criteria	*Ref.*
Fruits	Estimated phenotypic parameters of apples	Binocular stereo vision	$R^2 > 0.90$	(Ma et al., 2021)
	Modeling fruit (mandarin, orange, tomato) shape	Spheroid Models	–	(Albiol et al., 2021)
	3D reconstruction system for capturing, calibrating, and reconstructing fruits and tubers	Multi-view stereo	$R^2 > 0.97$ RMSE < 3	(Feldmann and Tabb, 2022)
	3D imaging system for strawberry phenotyping	multi-view stereo	RMSE < 3.97	(He et al., 2017)
	Volumetric estimation and grading of various fruits	Multiple camera views	RMSE < 0.77	(Jadhav et al., 2019)
	SFM as a viable option for fruit (tomato) with inadequate surface texture	SFM	$2.30 <$ RMSE < 2.44	*This work*
Plant	3D modeling of individual trees and accuracy assessment of height, stem diameter, and volume	SFM	$0.761 < R^2 < 0.98$	(Miller et al., 2015)
	Machine-vision-based height measurements for a cultivation robot	stereo vision	$0.78 < R^2 < 0.84$	(Kim et al., 2021)
Livestock	Weight-based body surface area measurements for pigs	SFM	$R^2 > 0.79$	(Pezzuolo et al., 2018)

editing, Validation, Formal analysis. **Rasool Khodabakhshian:** Writing – review & editing, Supervision, Project administration, Investigation, Funding acquisition.

Declaration of competing interest

The authors declare that they have no known competing financial interests or personal relationships that could have appeared to influence the work reported in this paper.

Data availability

Data will be made available on request.

Acknowledgment

The authors acknowledge and appreciate the funding and technical support provided by the Ferdowsi University of Mashhad, Iran, for this project.

References

Abd Rashid, A.N., Amir, F., Ramlan, S.A., Harron, N.A., Saod, A.H.M., 2020. Automated Asian fruit grading system using stereo vision technique. In: Journal of Physics: Conference Series. IOP Publishing, p. 12007.
Aguilar, M.a., Pozo, J.L., Aguilar, F.J., Sanchez-Hermosilla, J., Páez, F.C., Negreirosb, J., 2007. 3D surface modelling of tomato plants using close-range. Int. Arch. Photogramm. Remote. Sens. Spat. Inf. Sci. XXXVII, 139–144.
Ahmadabadian, A.H., Robson, S., Boehm, J., Shortis, M., Wenzel, K., Fritsch, D., 2013. A comparison of dense matching algorithms for scaled surface reconstruction using stereo camera rigs. ISPRS J. Photogramm. Remote Sens. 78, 157–167. https://doi.org/10.1016/j.isprsjprs.2013.01.015.
Albiol, A., Albiol, A., Sánchez de Merás, C., 2021. Fast 3D rotation estimation of fruits using spheroid models. Sensors 21, 2232.
Aldeeb, N.H., Hellwich, O., 2018. Reconstructing textureless objects-image enhancement for 3D reconstruction of weakly-textured surfaces. In: VISIGRAPP (5: VISAPP), pp. 572–580.
Andrade, G., Ramos, G., Madeira, D., Sachetto, R., Ferreira, R., Rocha, L., 2013. G-dbscan: A gpu accelerated algorithm for density-based clustering. Procedia Comput. Sci. 18, 369–378.
Ayob, N.Z.S., Kamarauzaman, N., Sahriman, N., 2015. Data acquisition for 3D surface modelling of chilli plant by using close range photogrammetry for volume estimation. In: 2015 IEEE Conference on Systems, Process and Control (ICSPC), IEEE, pp. 162–167.
Benos, L., Bechar, A., Bochtis, D., 2020. Safety and ergonomics in human-robot interactive agricultural operations. Biosyst. Eng. 200, 55–72. https://doi.org/10.1016/j.biosystemseng.2020.09.009.
Boari, F., Donadio, A., Schiattone, M.I., Cantore, V., 2015. Particle film technology: A supplemental tool to save water. Agric Water Manag 147, 154–162. https://doi.org/10.1016/j.agwat.2014.07.014.
Chen, M., Tang, Y., Zou, X., Huang, Z., Zhou, H., Chen, S., 2021. 3D global mapping of large-scale unstructured orchard integrating eye-in-hand stereo vision and SLAM. Comput. Electron. Agric. 187, 106237.
Chernov, V., Alander, J., Bochko, V., 2015. Integer-based accurate conversion between RGB and HSV color spaces. Comput. Electr. Eng. 46, 328–337.
Chiang, T., Fan, C.-P., 2018. 3D depth information based 2D low-complexity hand posture and gesture recognition design for human computer interactions. In: 2018 3rd International Conference on Computer and Communication Systems (ICCCS), IEEE, pp. 233–238.
Domis, M., Papadopoulos, A.P., Gosselin, A., 2002. Greenhouse tomato fruit quality. Hortic. Rev. 26, 239–349.
Dumas, Y., Dadomo, M., Di Lucca, G., Grolier, P., 2003. Effects of environmental factors and agricultural techniques on antioxidantcontent of tomatoes. J. Sci. Food Agric. 83, 369–382.
Edelman, G.J., Aalders, M.C., 2018. Photogrammetry using visible, infrared, hyperspectral and thermal imaging of crime scenes. Forensic Sci. Int. 292, 181–189.
Feldmann, M.J., Tabb, A., 2022. Cost-effective, high-throughput phenotyping system for 3D reconstruction of fruit form. Plant Phenome J. 5, e20029.
Feng, J., Teng, Q., Li, B., He, X., Chen, H., Li, Y., 2020. An end-to-end three-dimensional reconstruction framework of porous media from a single two-dimensional image based on deep learning. Comput. Methods Appl. Mech. Eng. 368, 113043.
Fuhrmann, S., Goesele, M., 2014. Floating scale surface reconstruction. ACM Trans. Graph. 33, 1–11.
Fuhrmann, S., Langguth, F., Moehrle, N., Waechter, M., Goesele, M., 2015. MVE—An image-based reconstruction environment. Comput. Graph. 53, 44–53.
Gharaghani, A., Mohammadi Javarzari, A., Vahdati, K., 2018. Kaolin particle film alleviates adverse effects of light and heat stresses and improves nut and kernel quality in Persian walnut. Sci. Hortic. (amsterdam) 239, 35–40. https://doi.org/10.1016/j.scienta.2018.05.024.
Glenn, D.M., 2012. The mechanisms of plant stress mitigation by kaolin-based particle films and applications in horticultural and agricultural crops. HortSci. 47, 710–711.
Glenn, D.M., Puterka, G.J., 2010. Particle films: a new technology for agriculture. Hortic. Rev. (am. Soc. Hortic. Sci). 31, 1–44.
He, J.Q., Harrison, R.J., Li, B., 2017. A novel 3D imaging system for strawberry phenotyping. Plant Methods 13, 1–8.
Herak, D., Mizera, C., Hrabe, P., Kabutey, A., 2018. 3D image analysis of the shapes and dimensions of several tropical fruits.
Hosseininaveh Ahmadabadian, A., Karami, A., Yazdan, R., 2019. An automatic 3D reconstruction system for texture-less objects. Rob. Auton. Syst. 117, 29–39. https://doi.org/10.1016/j.robot.2019.04.001.
Hu, K., Chen, Z., Kang, H., Tang, Y., 2024. 3D vision technologies for a self-developed structural external crack damage recognition robot. Autom. Constr. 159, 105262.
Hu, Y., Wang, L., Xiang, L., Wu, Q., Jiang, H., 2018. Automatic non-destructive growth measurement of leafy vegetables based on kinect. Sensors 18, 806.
Iglhaut, J., Cabo, C., Puliti, S., Piermattei, L., O'Connor, J., Rosette, J., 2019. Structure from motion photogrammetry in forestry: a review. Curr. for. Reports 5, 155–168.
Jadhav, T., Singh, K., Abhyankar, A., 2019. Volumetric estimation using 3D reconstruction method for grading of fruits. Multimed. Tools Appl. 78, 1613–1634.
Kench, S., Cooper, S.J., 2021. Generating three-dimensional structures from a two-dimensional slice with generative adversarial network-based dimensionality expansion. Nat. Mach. Intell. 3, 299–305.
Khojastehnazhand, M., Mohammadi, V., Minaei, S., 2019. Maturity detection and volume estimation of apricot using image processing technique. Sci. Hortic. (amsterdam) 251, 247–251.
Kim, W.S., Lee, D.H., Kim, Y.J., Kim, T., Lee, W.S., Choi, C.H., 2021. Stereo-vision-based crop height estimation for agricultural robots. Comput. Electron. Agric. 181, 105937 https://doi.org/10.1016/j.compag.2020.105937.
Kipli, K., Zen, H., Sawawi, M., Noor, M.S.M., Julai, N., Junaidi, N., Razali, M.I.S.M., Chin, K.L., Masra, S.M.W., 2018. Image processing mobile application for banana ripeness evaluation. In: 2018 International Conference on Computational Approach in Smart Systems Design and Applications (ICASSDA). IEEE, pp. 1–5.
Li, J., Teng, Q., Zhang, N., Chen, H., He, X., 2023. Deep learning method of stochastic reconstruction of three-dimensional digital cores from a two-dimensional image. Phys. Rev. E 107, 55309.
Lin, G., Tang, Y., Zou, X., Wang, C., 2021. Three-dimensional reconstruction of guava fruits and branches using instance segmentation and geometry analysis. Comput. Electron. Agric. 184, 106107.
Liu, J., Xu, X., Liu, Y., Rao, Z., Smith, M.L., Jin, L., Li, B., 2021. Quantitative potato tuber phenotyping by 3D imaging. Biosyst. Eng. 210, 48–59.
Lowe, D.G., 2004. Distinctive image features from scale-invariant keypoints. Int. J. Comput. Vis. 60, 91–110.
Ma, H., Zhu, X., Ji, J., Wang, H., Jin, X., Zhao, K., 2021. Rapid estimation of apple phenotypic parameters based on 3D reconstruction. Int. J. Agric. Biol. Eng. 14, 180–188.
Malekabadi, A.J., Khojastehpour, M., Emadi, B., 2019. Comparison of block-based stereo and semi-global algorithm and effects of pre-processing and imaging parameters on tree disparity map. Sci. Hortic. (amsterdam) 247, 264–274.
Marinoudi, V., Sørensen, C.G., Pearson, S., Bochtis, D., 2019. Robotics and labour in agriculture. A context consideration. Biosyst. Eng. 184, 111–121. https://doi.org/10.1016/j.biosystemseng.2019.06.013.
Meinen, B.U., Robinson, D.T., 2020. Mapping erosion and deposition in an agricultural landscape: optimization of UAV image acquisition schemes for SfM-MVS. Remote Sens. Environ. 239, 111666.
Miller, J., Morgenroth, J., Gomez, C., 2015. 3D modelling of individual trees using a handheld camera: Accuracy of height, diameter and volume estimates. Urban For. Urban Green. 14, 932–940.
Mon, T., ZarAung, N., 2020. Vision based volume estimation method for automatic mango grading system. Biosyst. Eng. 198, 338–349. https://doi.org/10.1016/j.biosystemseng.2020.08.021.
Naik, S., Patel, B., 2017. Machine vision based fruit classification and grading-a review. Int. J. Comput. Appl. 170, 22–34.
Nyalala, I., Okinda, C., Chao, Q., Mecha, P., Korohou, T., Yi, Z., Nyalala, S., Jiayu, Z., Chao, L., Kunjie, C., 2021. Weight and volume estimation of single and occluded tomatoes using machine vision. Int. J. Food Prop. 24, 818–832.
Omid, M., Khojastehnazhand, M., Tabatabaeefar, A., 2010. Estimating volume and mass of citrus fruits by image processing technique. J. Food Eng. 100, 315–321.
Palma, A., Cicilloni, A.M., Satta, D., De Pau, L., D'aquino, S., 2020. Effects of kaolin-based particle film on physiological, nutritional, nutraceuticals parameters and ceratitis capitata infestations in peach fruit at harvest and after storage. Adv. Hortic. Sci. 34, 81–88. https://doi.org/10.13128/ahsc-7669.
Paulus, S., Behmann, J., Mahlein, A.-K., Plümer, L., Kuhlmann, H., 2014. Low-cost 3D systems: suitable tools for plant phenotyping. Sensors 14, 3001–3018.
Pezzuolo, A., Milani, V., Zhu, D., Guo, H., Guercini, S., Marinello, F., 2018. On-barn pig weight estimation based on body measurements by structure-from-motion (SfM). Sensors 18, 3603.
Rahimi, M., Abbaspour-Fard, M.H., Rohani, A., 2022. Synergetic effect of N/O functional groups and microstructures of activated carbon on supercapacitor performance by machine learning. J. Power Sources 521, 230968. https://doi.org/10.1016/j.jpowsour.2021.230968.
Rupanagudi, S.R., Ranjani, B.S., Nagaraj, P., Bhat, V.G., 2014. A cost effective tomato maturity grading system using image processing for farmers. In: 2014 International Conference on Contemporary Computing and Informatics (IC3I), IEEE, pp. 7–12.
Sarafraz, A., Haus, B.K., 2016. A structured light method for underwater surface reconstruction. ISPRS J. Photogramm. Remote Sens. 114, 40–52.

Sharma, R.R., Datta, S.C., Varghese, E., 2020. Kaolin-based particle film sprays reduce the incidence of pests, diseases and storage disorders and improve postharvest quality of 'Delicious' apples. Crop Prot. 127, 104950 https://doi.org/10.1016/j.cropro.2019.104950.

Sofu, M.M., Er, O., Kayacan, M.C., Cetişli, B., 2016. Design of an automatic apple sorting system using machine vision. Comput. Electron. Agric. 127, 395–405.

Srivastava, S., Vani, B., Sadistap, S., 2020. Machine-vision based handheld embedded system to extract quality parameters of citrus cultivars. J. Food Meas. Charact. 14, 2746–2759.

Steeper, P., 2012. How to achieve accurate color from your camera. PSA J. 78, 18–20.

Thong, N.D., Thinh, N.T., Cong, H.T., 2019. Mango sorting mechanical system combines image processing. In: 2019 7th International Conference on Control, Mechatronics and Automation (ICCMA), IEEE, pp. 333–341.

Vivek Venkatesh, G., Iqbal, S.M., Gopal, A., Ganesan, D., 2015. Estimation of volume and mass of axi-symmetric fruits using image processing technique. Int. J. Food Prop. 18, 608–626.

Wang, Y., Chen, Y., 2020. Fruit morphological measurement based on three-dimensional reconstruction. Agronomy 10, 455.

Weerakkody, P., Jobling, J., Infante, M.M.V., Rogers, G., 2010. The effect of maturity, sunburn and the application of sunscreens on the internal and external qualities of pomegranate fruit grown in Australia. Sci. Hortic. (amsterdam) 124, 57–61. https://doi.org/10.1016/j.scienta.2009.12.003.

Yahaya, S., Jikan, S.S., Badarulzaman, N.A., Adamu, A.D., 2017. Chemical composition and particle size analysis of kaolin. Path Sci. 3, 1001–1004. https://doi.org/10.22178/pos.27-1.

Yamamoto, S., Karkee, M., Kobayashi, Y., Nakayama, N., Tsubota, S., Thanh, L.N.T., Konya, T., 2018. 3D reconstruction of apple fruits using consumer-grade RGB-depth sensor. Eng. Agric. Environ. Food 11, 159–168.

Ye, L., Wu, F., Zou, X., Li, J., 2023. Path planning for mobile robots in unstructured orchard environments: An improved kinematically constrained bi-directional RRT approach. Comput. Electron. Agric. 215, 108453.

Zine-El-Abidine, M., Dutagaci, H., Galopin, G., Rousseau, D., 2021. Assigning apples to individual trees in dense orchards using 3D colour point clouds. Biosyst. Eng. 209, 30–52.